Laboratory evidence for Krauklis wave resonance in a fracture and implications for seismic coda wave analysis

Pei-Ju Rita Shih (ETH Zurich) and Marcel Frehner (ETH Zurich)*

Summary

Krauklis waves are of major interest since they can lead to resonance effects in fluid-filled fractured rocks and may reveal the properties of reservoir rocks. A previous numerical study demonstrates that body waves are capable of initiating Krauklis waves and that the initiation strongly depends on the incident wave mode (P- or S-wave) and fracture orientation. It also shows that incident S-waves may carry more information about fractures. Here we present a laboratory study that simulates similar conditions as in the numerical experiments of a homogenous medium containing a single well-defined fracture. We record the signals obtained from propagating ultrasonic waves along a sample without a fracture and samples with a fracture with different inclination angles of 30°, 45°, and 60°. The experimental results of an incident S-wave indicate that the presence of the fracture leads to resonance effects, which decay over time in the recorded seismic coda at frequencies lower than the dominant source frequency, i.e. at approximately 0.1 MHz. The resonance frequency is independent of the fracture orientation and the source frequency. We interpret this effect as a resonance in the fracture, whose resonance frequency is an intrinsic property of the fracture size and elastic properties. In addition, we plan to employ an analytical solution to verify our laboratory results by investigating the relationship between the fracture width, fracture length, resonance frequency, and quality factor. We aim to identify relationships between the recorded seismic signal and the fracture properties (e.g., geometry, orientation, and fluid type).

Introduction

The Krauklis wave is a unique guided seismic wave mode, which is bound to fluid-filled fractures and propagates along such fractures (Krauklis, 1962). It is highly dispersive with a low phase velocity at low frequencies in a system of a fluid bounded by two elastic half-spaces with different material properties (Ferrazzini and Aki, 1987; Chouet, 1996; Ashour, 2000; Korneev, 2008; Korneev, 2009; Korneev, 2010). It is expected to be able to resonate in the fracture and hence emit seismic signals with a signature frequency. This resonant behavior should lead to strong frequency dependence for seismic body waves, enabling the identification of Krauklis wave-related signals in the coda of recorded seismograms (Korneev, 2008).

Aki et al. (1977), Chouet (1988), and Chouet (1996) used this resonance behavior to show the potential of volcanic eruption forecasting by recording long-period volcanic tremor signals, which provide information of the state of fluid in the subsurface. Tary et al. (2014) identified and interpreted the observed resonances during hydraulic fracturing activities. The recorded frequency content contains useful information for understanding the reservoir formation. The characteristics of Krauklis waves might be one of the keys to reveal properties of fluid-bearing fractured rocks.

Korneev (2009) suggested that Krauklis waves might be an important phenomenon to understand the observed frequency-dependent and nonlinear behavior of fluid reservoirs. Several theoretical studies have analytically derived the dispersion behavior of Krauklis waves in infinitely long and straight fractures (e.g., Korneev, 2008). Frehner and Schmalholz (2010) state that the resonance behavior of Krauklis waves in fractures should be incorporated into effective medium theories in order to obtain more realistic models for fractured rocks. However, purely analytical methods cannot handle realistic fracture geometries or finite-length fractures. Therefore, we combine numerical modeling results with laboratory experiments to visualize fracture-related effects on seismic wave propagation in reservoir rocks.

The Krauklis wave cannot be detected at a relatively short distance away from the fracture because of the exponential decay of their amplitude in space. Frehner and Schmalholz (2010) demonstrated that Krauklis waves can be detected as a converted body wave as a result of scattering at the crack tips and at irregularities of the fracture. The study also shows that the reflection behavior of Krauklis wave depends significantly on different crack geometries and different fluids in the crack. Moreover, Frehner (2014) employed a 2D finite-element model to demonstrate that both P- and S-waves are capable of initiating Krauklis waves. The fracture-internal oscillatory behavior of Krauklis waves can be converted to body waves and transmitted into the surrounding rock, which allows it to be detected away from the fracture.The initiation of Krauklis waves by body waves strongly depends on the incident angle and on the incident wave mode (P- or S-wave). The study shows that incident S-waves initiate larger amplitude Krauklis waves than P-waves. As a result, S-waves may carry more information about fractures such as fracture orientation or fluid content. The following laboratory study focuses mainly on the case of an incident S-wave. The numerical setup of Frehner (2014) provides the guidelines for our laboratory investigation.

Laboratory Configuration

A cylindrical Plexiglas sample (120 mm length, 25 mm diameter) containing a single fracture (Figure 1a) is chosen as the ideal material to mimic the simplified numerical setup. A 0.1 mm thick fracture is manufactured by cutting the sample at a given angle, milling on one side a 0.1 mm deep, 25 x 15 mm elliptical hole, and fusing the two pieces back together with chloroform (Figure 1a, b). Chemically fusing the Plexiglas with chloroform leads to an isolated fracture without interfaces around the fracture. Following this procedure, we created samples with fractures at 30°, 45°, and 60° inclination angles. We employ the ultrasonic pulse transmission method (source at position 1; receiver at position 2 in Figure 1a). The P-wave transducers are screwed embedded in the Plexiglas sample; the S-wave setup is slightly different due to the transducer's configuration. Figure 1c illustrates the experimental setup for both P-wave and S-wave acquisition.

Laboratory Results

The seismic signal is recorded and transformed into the frequency domain by a Fast Fourier Transform. The seismic signal is further converted into spectrograms.

Figure 2 displays the receiver spectra for an S-wave source with 1 MHz source frequency for the intact sample and for fractured samples with 30°, 45°, and 60° inclination angles, respectively. The general patterns of the receiver spectrum are similar for all four experiments. However, a fracture-related attenuation can be identified at around 0.1 MHz for all three different inclination angles. The receiver spectrum for the case of 45° fracture inclination reveals the largest attenuation as compared to the cases of 30° and 60° (Figure 2).

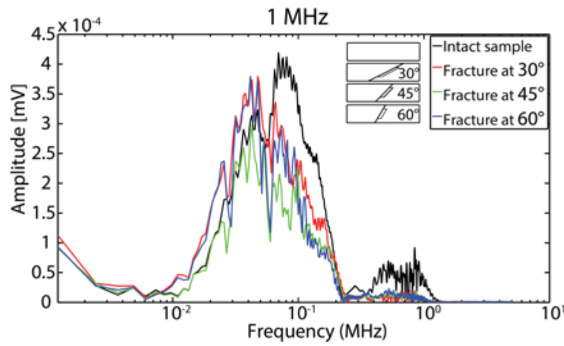

Figure 2: Receiver spectra for experiments with a dominant S-wave source frequency of 1 MHz for the intact sample and fractured samples with a fracture inclination angle of 30°, 45°, and 60°.

Figure 3 presents the spectrograms of the receiver data. The presence of the fracture induces elevated amplitudes at low frequencies in the coda after the first arrival (150 µs onwards, Figure 3b, c, and d). The spectrogram for the case of 45° fracture inclination exhibits relatively larger amplitude around 0.1 MHz (200 µs, Figure 3c) as compared to the cases of 30° and 60°. This fracture-related effect is very narrow-banded (around 0.1 MHz) and decays relatively slowly. The resonance frequency is independent of the fracture orientation and of the used source frequency (not shown here).

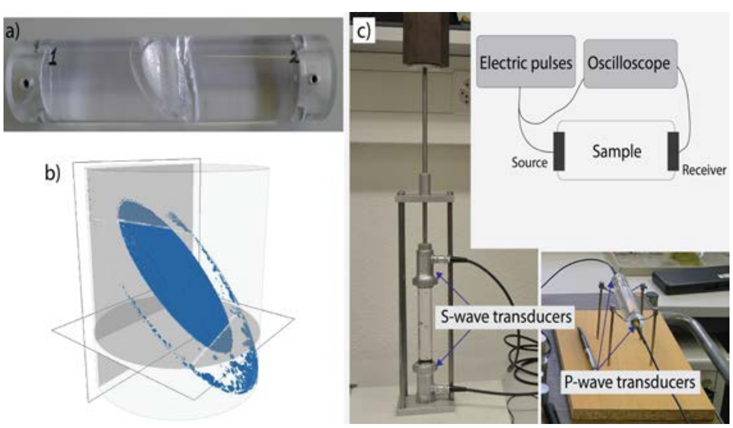

Figure 1: a) Plexiglas sample (120 mm length, 25 mm diameter) with manufactured elliptical fracture (25 x 15 mm, 0.1 mm thickness, 45° inclination angle) for P-wave acquisition. b) Segmented micro-CT scan of the same sample (transparent grey) containing the manufactured fracture (blue). c) Left: S-wave acquisition setup. The sample is placed between the S-wave transducers under a custom-made presser with a metal weight, which enhances the coupling between the sample and the transducers. Bottom right: P-wave acquisition setup. The sample is hung on top of two cotton wires to obtain the smallest possible contact surface between the sample and the means of suspension, minimizing the contact effects. The P-wave transducers are screwed embedded in the Plexiglas sample. Top right: For both setups, one transducer is connected to the electric pulser (source) and the other is connected to the oscilloscope (receiver).

Laboratory evidence for Krauklis wave resonance in a fracture

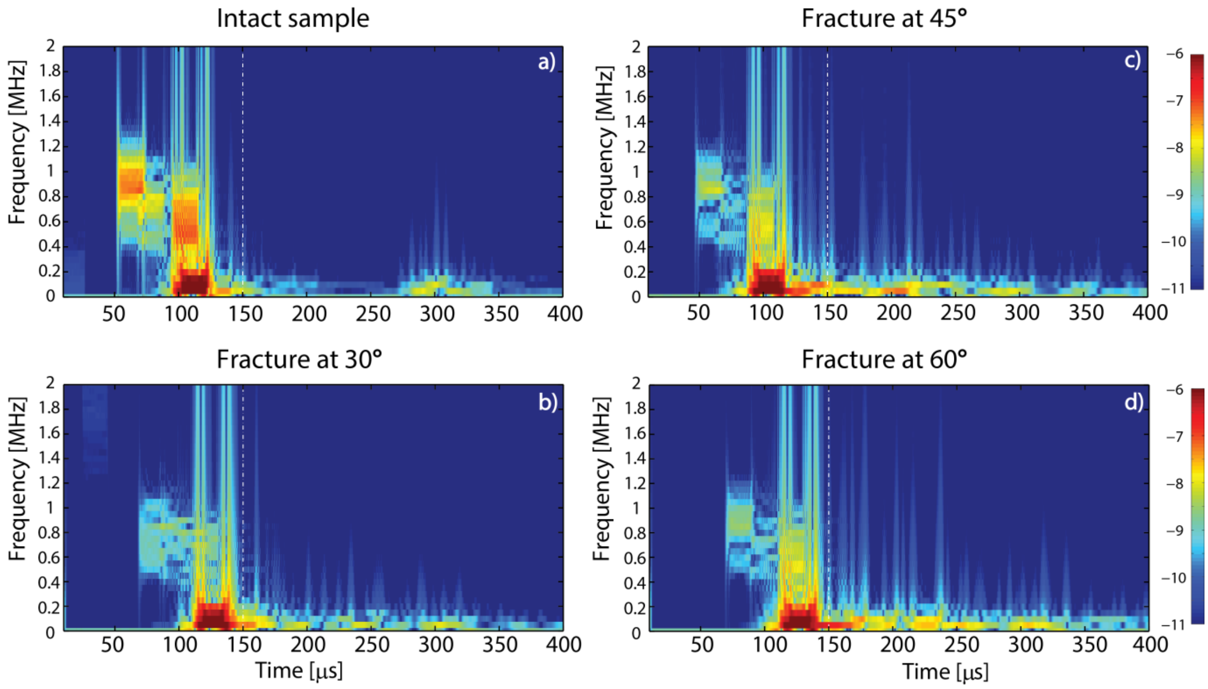

Figure 3: Spectrograms of receiver time signals generated by an S-wave with a source frequency of 1 MHz propagating through the intact sample (a) ,and fractured samples with a fracture inclination angle of 30° (b), 45° (c), and 60° (d), respectively.

Discussion and Outlook

The main amplitude of the spectra (Figure 2) is not concentrated at the source frequency (1 MHz) due to the intrinsic attenuation of Plexiglas. We repeated the measurements using a reduced sample length to counter against this loss; yet the spectra are identical to the spectra of the original length (120 mm).

Of course there are differences between the numerical setup (Frehner, 2014) and the laboratory setup, such as the source and receiver positions, the filling of the fracture (here: air), and the source frequency range. Despite the different setups, our preliminary laboratory results coincide with the published numerical results (Frehner, 2014) where we expect the largest effect of the fracture in the case of an incident S-wave at an inclination angle of 45°.

The presence of a fracture with three different inclination angles leads to a possible resonance effect around 0.1 MHz. Because this effect is very narrow banded, decays slowly after the arrival of the direct wave, and is independent of the fracture orientation, we interpret the enhanced amplitude to be due to oscillating Krauklis waves in the fracture, whose resonance frequency is an intrinsic property of the fracture geometry and elastic properties.

In the future, we will focus on predicting the fracture orientation from the recorded receiver signals by quantifying the difference between the spectrograms for different fracture orientations. Our ongoing laboratory experiments might demonstrate a relationship between the measured resonance effect (frequency and decay of resonance) and fracture properties (length, aperture, orientation, fluid content), which will be further verified with an analytical solution. Further on, we plan to measure a wider range of inclination angles and dimensions of the fracture. Eventually, we will employ natural samples, which are more representative of natural fractured reservoirs.

Analytical solution

Lipovsky and Dunham (2015) provide an analytical solution for estimating the aperture and length of a hydraulic fracture by using the seismically observed characteristic resonance frequency and temporal quality factor. Fluid viscosity and emitted seismic energy are the two attenuation mechanisms for gradual amplitude decay in

Laboratory evidence for Krauklis wave resonance in a fracture

the coda (Aki, 1984; Chouet, 1992). The attenuation in the model of Lipovsky and Dunham (2015) is due to fluid viscosity alone.

In the crack wave limit, the fluid is incompressible and fluid flow pushes the conduit walls apart (Figure 4a). In the sound wave limit, the walls are rigid and fluid flow compresses the fluid and increases the fluid density (Figure 4b). Depending on the fluid type, these two flow regimes can be further divided. For our laboratory setup, the Plexiglas is rigid as compared to air, which is a highly compressible fluid.

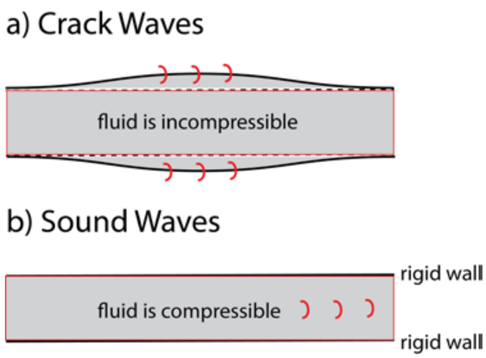

Figure 4: a) The fluid is effectively incompressible and fluid flow pushes the conduit walls apart. The guided wave travels along the fracture wall. b) The conduit walls are effectively rigid. The guided wave travels within the fluid. (redrawn from Lipovsky and Dunham, 2015)

Relationship of fracture width and length with resonant frequency and quality factor

Equations 1 and 2 (Lipovsky and Dunham, 2015) are the general expressions relating the fracture geometry to the characteristic resonant frequency f and quality factor Q:

$$L = \frac{1}{2}\left[\pi \nu \left(\frac{G}{\rho}\right)^2 \frac{Q^2}{f^5}\right]^{1/6}, \quad (1)$$

$$2w = Q\sqrt{\nu/(\pi f)}, \quad (2)$$

where L is the fracture length, ν is the kinematic viscosity, G is the elastic plane strain modulus, ρ is the fluid density, and w is the unperturbed facture half width. Using these equations, the characteristic resonant frequency f and quality factor Q uniquely constrain the fracture geometry if the fluid and solid mechanical properties are known.

Lipovsky and Dunham (2015) visualize a more complete solution of these general expressions by a graphical method (Figure 5). In natural geological systems, the resonant characteristic frequency f is in the range of 1 to 1000 Hz. Figure 5 represents the relationship between fracture geometry (half-width and length), quality factor (black contour lines), and characteristic frequency (red contour lines).

The source frequency range for our experiments is from 0.225 MHz to 5 MHz. In the next step, we plan to employ the analytical solution to construct a similar graphical solution (Figure 5) in order to verify our experimental results.

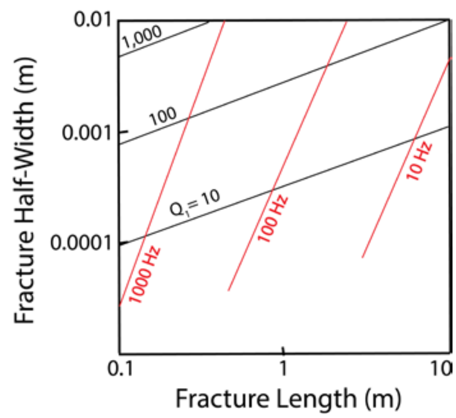

Figure 5: Inferred fracture half-width and length of hydraulic fractures from observed seismic frequency f and quality factor Q. (redrawn from Lipovsky and Dunham, 2015)

Conclusions

Our laboratory results show that the presence of the fracture leads to possible resonance effects with a characteristic frequency different from the source frequency, which we interpret to be caused by Krauklis waves propagating back and forth along the fracture. The resonance frequency is independent of the fracture orientation and source frequency; hence it is an intrinsic property of the fracture geometry and mechanical properties.

We conclude that seismic coda, in particular of S-wave experiments, may contain useful information about the intrinsic fracture properties.

Acknowledgment

We acknowledge the support by the Swiss National Science Foundation (project UPseis, 200021_143319).

References

Aki, K., 1984, Evidence for magma intrusion during the Mammoth Lakes earthquakes of May 1980 and implications of the absence of volcanic (harmonic) tremor: Journal of Geophysical Research, **89**, 7689–7696, doi: 10.1029/JB089iB09p07689.

Aki, K., M. Fehler, and S. Das, 1977, Source mechanism of volcanic tremor: Fluid-driven crack models and their application to the 1963 Kilauea eruption: Journal of Volcanology and Geothermal Research, **2**, 259–287.

Ashour, A. S., 2000, Wave motion in a viscous fluid-filled fracture: International Journal of Engineering Science, **38**, 505–515, doi: 10.1016/S0020-7225(99)00045-2.

Chouet, B., 1988, Resonance of a fluid-driven crack: Radiation properties and implications for the source of long-period events and harmonic tremor: Journal of Geophysical Research, **93**, 4375–4400, doi: 10.1029/JB093iB05p04375.

Chouet, B., 1992, A seismic model for the source of long-period events and harmonic tremor, in P. Gasparini, R. Scarpa, and K. Aki, eds., Volcanic Seismology: IAVCEI Proceedings in Volcanology: Berlin, Heidelberg, New York, Springer-Verlag, 133-156.

Chouet, B., 1996, Long-period volcano seismicity: Its source and use in eruption forecasting: Nature, **380**, 309–316, doi: 10.1038/380309a0.

Ferrazzini, V., and K. Aki, 1987, Slow waves trapped in a fluid-filled infinite crack: Implication for volcanic tremor: Journal of Geophysical Research, **92**, 9215–9223, doi: 10.1029/JB092iB09p09215.

Frehner, M., and S. M. Schmalholz, 2010, Finite-element simulations of Stoneley guided-wave reflection and scattering at the tips of fluid-filled fractures: Geophysics, **75**, no. 2, T23–T36, doi: 10.1190/1.3340361.

Frehner, M., 2014, Krauklis wave initiation in fluid-filled fractures by seismic body waves: Geophysics, **79**, no. 1, T27-T35, doi: 10.1190/GEO2013-0093.1.

Korneev, V., 2008, Slow waves in fractures filled with viscous fluid: Geophysics, **73**, no. 1, N1–N7, doi:10.1190/1.2802174.

Korneev, V. A., A. A. Ponomarenko, and M. Kashtan, 2009, Stoneley guided waves: What is missing in Biot's theory?, in H. I. Ling, A. Smyth, and R. Betti, eds., Poromechanics IV: Proceedings of the fourth Biot conference on poromechains: DEStech Publications Inc., 706-711.

Korneev, V., 2010, Low-frequency fluid waves in fractures and pipes: Geophysics, **75**, no. 6, N97–N107, doi: doi:10.1190/1.3484155.

Krauklis, P. V., 1962, About some low frequency oscillations of a liquid layer in elastic medium: Prikladnaya Matematika i Mekhanika, **26**, 1111-1115.

Lipovsky, B. P., and E. M. Dunham, 2015, Vibrational modes of hydraulic fractures: Inference of facture geometry from resonant frequencies and attenuation: Journal of Geophysical Research, **120**, 1080-1107, doi: 10.1002/2014JB011286.

Tary, J. B., M. van der Baan, and D. W. Eaton, 2014, Interpretation of resonance frequencies recorded during hydraulic fracturing treatments: Journal of Geophysical Research, **119**, 1295-1315, doi: 10.1002/2013JB010904.